



Government  
of Canada

Gouvernement  
du Canada

Canada

---

# **Full-Scale Wind-Tunnel Simulation of Takeoff Performance Degradation with Contaminated Fluid Runback**

---

TP 13925E

April 2002

Prepared for  
Transportation Development Centre  
Transport Canada

by  
National Research Council Canada  
Institute for Aerospace Research  
Aerodynamics Laboratory  
Ottawa, Ontario



**Full-Scale Wind-Tunnel Simulation of  
Takeoff Performance Degradation  
with Contaminated Fluid Runback**

by  
Myron M. Oleskiw  
Paul J. Penna  
Richard S. Crabbe  
Martin E. Beyers  
National Research Council Canada  
Institute for Aerospace Research  
Aerodynamics Laboratory  
Ottawa, Ontario

April 2002

This report reflects the views of the authors and not necessarily those of the Transportation Development Centre of Transport Canada.

The Transportation Development Centre does not endorse products or manufacturers. Trade or manufacturers' names appear in this report only because they are essential to its objectives.

Un sommaire français se trouve avant la table des matières.



1. Transport Canada Publication No. <b>TP 13925E</b>		2. Project No. <b>9033 (DC 143)</b>		3. Recipient's Catalogue No.	
4. Title and Subtitle <b>Full-Scale Wind-Tunnel Simulation of Takeoff Performance Degradation with Contaminated Fluid Runback</b>				5. Publication Date <b>April 2002</b>	
				6. Performing Organization Document No.	
7. Author(s) <b>Myron M. Oleskiw, Paul J. Penna, Richard S. Crabble, Martin E. Beyers</b>				8. Transport Canada File No. <b>ZCD2450-B-14</b>	
9. Performing Organization Name and Address <b>National Research Council Canada Institute for Aerospace Research, Aerodynamics Laboratory Montreal Road Ottawa, Ontario K1A 0R6</b>				10. PWGSC File No.	
				11. PWGSC or Transport Canada Contract No.	
12. Sponsoring Agency Name and Address <b>Transportation Development Centre (TDC) 800 René Lévesque Blvd. West Suite 600 Montreal, Quebec H3B 1X9</b>				13. Type of Publication and Period Covered <b>Final</b>	
				14. Project Officer <b>Barry B. Myers</b>	
15. Supplementary Notes (Funding programs, titles of related publications, etc.) <b>Co-sponsored by Transport Canada's Civil Aviation directorate and by National Research Council Canada's Institute for Aerospace Research. This report is based on a paper presented at the American Helicopter Society/SAE International Icing Symposium '95 in Montreal, Quebec, Canada, September 18-21, 1995.</b>					
16. Abstract <p>In response to the problem of wintertime precipitation contamination, manufacturers have developed freezing point depressant (FPD) fluids for application to the aircraft's lifting and control surfaces, and which are designed to be shed from these surfaces during the takeoff run. An exploratory investigation was conducted to estimate the aerodynamic performance penalties produced by residual de- and anti-icing fluids. This investigation included experiments using both neat and diluted fluids as well as fluids that had been contaminated by freezing precipitation.</p> <p>The experiments were carried out in the National Research Council Canada's 3 m x 6 m open circuit Propulsion Wind Tunnel. The model was a two-dimensional, single-element NACA 23012 aerofoil of 1.5 m chord. The tests involved simulated takeoff roll and rotation. The investigation showed that the flow of anti-icing fluids during the take-off roll and rotation was dominated by waves with a height of about 0.5 mm. These waves produced a small, temporary lift loss during rotation, with no significant impact on the model's stall characteristics. The contamination of anti-icing fluids by freezing precipitation resulted in a decrease in the aerofoil stall margin of up to 3.3 deg with a lift loss of up to 9.8 percent just prior to stall. The growth of a layer of frost on a simulated cold-soaked unprotected aerofoil caused a decrease in stall margin of 4.5 deg, with a lift loss of approximately 18.6 percent.</p>					
17. Key Words <b>Aerodynamic behaviour, airfoil, de/anti-icing fluids, wind tunnel tests</b>			18. Distribution Statement <b>Limited number of copies available from the Transportation Development Centre</b>		
19. Security Classification (of this publication) <b>Unclassified</b>	20. Security Classification (of this page) <b>Unclassified</b>	21. Declassification (date) <b>—</b>	22. No. of Pages <b>x, 16</b>	23. Price <b>Shipping/ Handling</b>	



1. N° de la publication de Transports Canada TP 13925E		2. N° de l'étude 9033 (DC 143)		3. N° de catalogue du destinataire		
4. Titre et sous-titre Full-Scale Wind-Tunnel Simulation of Takeoff Performance Degradation with Contaminated Fluid Runback				5. Date de la publication Avril 2002		
				6. N° de document de l'organisme exécutant		
7. Auteur(s) Myron M. Oleskiw, Paul J. Penna, Richard S. Crabble, Martin E. Beyers				8. N° de dossier - Transports Canada ZCD2450-B-14		
9. Nom et adresse de l'organisme exécutant Conseil national de recherches du Canada Institut de recherche aérospatiale, Laboratoire d'aérodynamique Montreal Road Ottawa, Ontario K1A 0R6				10. N° de dossier - TPSGC		
				11. N° de contrat - TPSGC ou Transports Canada		
12. Nom et adresse de l'organisme parrain Centre de développement des transports (CDT) 800, boul. René-Lévesque Ouest Bureau 600 Montréal (Québec) H3B 1X9				13. Genre de publication et période visée Final		
				14. Agent de projet Barry B. Myers		
15. Remarques additionnelles (programmes de financement, titres de publications connexes, etc.) Coparrainée par la Direction générale de l'aviation civile de Transports Canada et l'Institut de recherche aérospatiale du Conseil national de recherches du Canada. Ce rapport est inspiré d'une communication présentée au <i>American Helicopter Society/SAE International Icing Symposium '95</i> , tenu à Montréal, Québec, Canada, du 18 au 21 septembre 1995.						
16. Résumé <p>En marge de leurs efforts pour résoudre le problème de la contamination des aéronefs par des précipitations hivernales, les fabricants ont mis au point des fluides abaisseurs du point de congélation. Ceux-ci sont conçus pour être appliqués sur les surfaces portantes et les gouvernes des aéronefs, et être ensuite chassés de ces surfaces pendant la course au décollage. Une recherche exploratoire a été menée afin d'évaluer dans quelle mesure les fluides dégivrants/antigivrage qui demeurent sur les surfaces dégradent le comportement aérodynamique de l'aéronef. Diverses expériences ont mis en jeu des fluides dilués et non dilués, et des fluides contaminés par des précipitations givrantes.</p> <p>Ces expériences ont eu lieu dans la soufflerie à propulsion à boucle ouverte de 3 m sur 6 m du Conseil national de recherches du Canada. Un profil de voilure bidimensionnel à un élément NACA 23012, de 1,5 m de corde, a servi aux essais. Ceux-ci, qui consistaient à simuler la course au décollage et la rotation, ont révélé que les fluides dégivrants/antigivrage produisaient, en s'écoulant sur les surfaces, des ondulations d'une hauteur d'environ 0,5 mm. Ces ondulations entraînaient une perte de portance légère et momentanée lors de la rotation, mais n'avaient aucun effet significatif sur les paramètres de décrochage de l'aile. Lorsque les fluides antigivrage étaient contaminés par des précipitations givrantes, les chercheurs ont noté une diminution de la marge de décrochage de l'aile atteignant 3,3 degrés, et une diminution allant jusqu'à 9,8 p. 100 de la portance, immédiatement avant le décrochage. Par comparaison, l'accumulation de givre sur une maquette d'aile sur-refroidie non protégée a entraîné une diminution de la marge de décrochage de 4,5 degrés et une perte de portance d'environ 18,6 p. 100.</p>						
17. Mots clés Comportement aérodynamique, surface portante, fluides dégivrants/antigivrage, essais en soufflerie				18. Diffusion Le Centre de développement des transports dispose d'un nombre limité d'exemplaires.		
19. Classification de sécurité (de cette publication) Non classifiée		20. Classification de sécurité (de cette page) Non classifiée		21. Déclassification (date) —	22. Nombre de pages x, 16	23. Prix Port et manutention

## **ACKNOWLEDGEMENTS**

This study was funded in part by the Transport Canada Aviation – Dryden Commission Implementation Project. The authors wish to thank Barry Myers and Frank Eyre, the Scientific Authorities, for their helpful discussions and cooperation.

Acknowledgements are due to Instrumar Ltd. and AlliedSignal Aerospace Canada for their help with the contaminant and fluid integrity system. We also wish to thank Dr. Robert Gagnon (developer of the laser fluid/ice depth measurement technique) and Dave Marcotte of National Research Council Canada for their assistance with the fluid depth measurement instrumentation; the Max Kurowski Aviation Group for helping with the design of a FPD fluid spreading device; and Octagon Process, Inc. and Union Carbide Inc. for providing FPD fluids for use during the experiments.





## **SUMMARY**

An exploratory investigation was conducted to estimate the aerodynamic performance penalties produced by de- and anti-icing fluids. This investigation included experiments using both neat and diluted fluids as well as fluids that had been contaminated by freezing precipitation.

The experiments were carried out in National Research Council Canada's 3 m x 6 m open circuit Propulsion Wind Tunnel. The model was a two-dimensional, single-element NACA 23012 aerofoil of 1.5 m chord. The investigation showed that the flow of anti-icing fluids during the take-off roll and rotation was dominated by waves with a height of about 0.5 mm. These waves produced a small, temporary lift loss during rotation, with no significant impact on the model's stall characteristics. The contamination of anti-icing fluids by freezing precipitation resulted in a decrease in the aerofoil stall margin of up to 3.3 deg with a lift loss of up to 9.8 percent just prior to stall. The growth of a layer of frost on a simulated cold-soaked unprotected aerofoil caused a decrease in stall margin of 4.5 deg, with a lift loss of approximately 18.6 percent. The application of results such as these to the future refinement of airline operations and aviation regulations could lead to safer operations under ground icing conditions.

## SOMMAIRE

Une recherche exploratoire a été menée pour étudier la dégradation des performances aérodynamiques de surfaces portantes attribuable aux fluides antigivrage. Cette recherche comportait des essais à l'aide de fluides dilués et non dilués, et de fluides contaminés par des précipitations givrantes.

Les expériences ont eu lieu dans la soufflerie à propulsion à boucle ouverte de 3 m sur 6 m du Conseil national de recherches du Canada. La maquette utilisée était un profil de voilure bidimensionnel à un élément NACA 23012, de 1,5 m de corde. Les essais ont révélé que les fluides dégivrants/antigivrage produisaient, en s'écoulant sur les surfaces lors de la course au décollage et de la rotation, des ondulations d'une hauteur d'environ 0,5 mm. Ces ondulations entraînaient une perte de portance légère et momentanée lors de la rotation, mais n'avaient aucun effet significatif sur les paramètres de décrochage de l'aile. Lorsque les fluides antigivrage étaient contaminés par des précipitations givrantes, les chercheurs ont noté une diminution de la marge de décrochage de l'aile atteignant 3,3 degrés et une diminution allant jusqu'à 9,8 p. 100 de la portance, immédiatement avant le décrochage. Par comparaison, l'accumulation de givre sur une maquette d'aile sur-refroidie non protégée a entraîné une diminution de la marge de décrochage de 4,5 degrés et une perte de portance d'environ 18,6 p. 100. La prise en compte de ces résultats lors des révisions futures de la réglementation du transport aérien devrait contribuer à rendre plus sûres les opérations aériennes en conditions de givrage au sol.

## TABLE OF CONTENTS

Introduction .....	1
Background.....	1
Propulsion Wind Tunnel .....	2
Wing Model and Support.....	2
Instrumentation and Data Acquisition .....	4
Fluid Application .....	4
Freezing Precipitation Simulation .....	5
Flow Visualization.....	6
Experiment Matrix .....	7
Clean Wing Aerodynamics .....	8
De-/Anti-Icing Fluid Flow Behaviour and Its Aerodynamic Effects .....	9
Aerodynamic Effects of Freezing Precipitation .....	10
Aerodynamic Effects of Freezing Precipitation on De-/Anti-Icing Fluids .....	10
Aerodynamic Effects of Frost Formation .....	12
Summary of Aerodynamic Effects .....	12
Conclusions.....	13
References.....	15

## LIST OF FIGURES

Figure 1	A schematic diagram of the wing model used in the experiments. ....	3
Figure 2	A schematic view of the upper half of the test section showing the location of the wing model, the freezing rain simulator and the photographic systems.....	5
Figure 3.	The wand-like device used for evenly spreading the de- and anti-icing fluids on the wing. ....	6
Figure 4	Lift and moment coefficients vs. angle of attack for a clean wing.....	8
Figure 5	Lift and moment coefficients vs. angle of attack for a Type II fluid diluted 50/50.....	9
Figure 6	Lift and moment coefficients vs. angle of attack for a layer of ice formed by rain on a cold-soaked wing. ....	10
Figure 7	Lift and moment coefficients vs. angle of attack for a layer of ice formed following the failure of a layer of neat Type II fluid. ....	11
Figure 8	Lift and moment coefficients vs. angle of attack for a layer of frost and a partially sublimated layer of frost (labelled Light Frost).....	12
Figure 9	Changes in the maximum lift coefficient as a function of wing contaminant and air and wing temperatures. ....	13
Figure 10	Changes in the stall angle as a function of wing contaminant and air and wing temperatures.....	14

## **Introduction**

Recent aircraft accidents attributed to ground icing have heightened concerns about winter operations of commercial aircraft, underscoring the importance of an adequate understanding of the phenomenon.

Previous studies have focused on the aerodynamic performance effects of some Type I (de-icing) and Type II (anti-icing) fluids on wind tunnel models and on aircraft wings in flight tests (Refs. 2 through 6). Two of these studies reported measurable lift loss and drag increase. The third found small performance losses in some cases, but none were sufficient to result in aircraft operational advisories. The authors are not aware of any studies which have quantified the aerodynamic impact of such fluids once they have been contaminated by freezing precipitation. Therefore, an exploratory wind tunnel investigation using a single element aerofoil was carried out.

With the support of the Dryden Commission Implementation Project of Transport Canada, the National Research Council of Canada (NRC) performed a series of exploratory experiments in its 3 m x 6 m Propulsion Wind Tunnel (PWT) with the following objectives:

1. Estimation of the aerodynamic performance degradation effects of a variety of neat and diluted de-/anti-icing fluid types at temperatures near the freezing point.
2. Documentation of the flow of de- and anti-icing fluids during a simulated aircraft takeoff roll and rotation.
3. Estimation of the level of aerofoil aerodynamic performance degradation due to de- and anti-icing fluids contaminated to the end of their holdover time.
4. Assessment of the ability of the holdover times obtained through the use of inclined flat plate tests to predict the times required to contaminate the fluids to the point of significant impact on wing aerodynamics.

Given the short lead time for preparing and performing the experiments prior to the end of the 1994-95 winter season, the experiments were designed to test the feasibility of obtaining useful aerodynamic performance degradation results from a near full-scale wing model in a wind tunnel following fluid application and freezing precipitation contamination.

## **Background**

The safety of aircraft operations is compromised by three types of aircraft lifting and control surface contamination: ice accretion due to in-flight icing; frost formation due primarily to cold fuel in aircraft wing tanks and adhesion of wintertime precipitation prior to aircraft takeoff. The hazards of all three types of contamination have been recognized for a number of years, but recent accidents in Canada (Air Ontario Fokker F-28 at Dryden in March 1989, Ref. 1) and the United States (US Air Fokker F-28 at LaGuardia in March 1992) have heightened awareness of the problem of wintertime precipitation accumulation and adherence on the ground.

In response to the problem of wintertime precipitation contamination, a number of manufacturers have developed freezing point depressant (FPD) fluids for application to the aircraft's lifting and control surfaces prior to takeoff. Such fluids fall into two primary categories:

1. SAE Type I fluid, typically an ethylene- or propylene-glycol and water mixture, usually applied to the aircraft at elevated temperatures to remove any precipitation adhering to the aircraft's surfaces.
2. SAE Type II fluid, similar to Type I but with polymers added to increase the viscosity of the fluid at the time of application thus allowing the fluid to remain on the aircraft during taxiing. The fluid viscosity diminishes during the shearing action of the airflow over the wing during takeoff.

The aerodynamic effects on aircraft performance of the Type I and II fluids have been investigated by full-scale aircraft tests (Refs. 2 and 3) and in two-dimensional and three-dimensional wind tunnel tests (Refs. 4, 5, 6 and 7). No such tests have yet been performed on the more recently developed Type II fluids which have even higher viscosity at the time of application.

Work by the SAE G-12 Holdover Time Working Group during the last several winters has focused upon attempting to substantiate the holdover times for various types of de- and anti-icing fluids under natural and laboratory simulated precipitation conditions (Refs. 8 and 9). Because of the difficulties and costs associated with testing of these fluids on full-size aircraft wings, a procedure was developed to do the testing on inclined flat plates. While United Airlines performed some tests comparing visual-failure holdover times for aircraft wings versus the flat plates in Denver (Ref. 10), there remains some uncertainty in the aviation community as whether the holdover times derived from the flat plate tests truly represent those for aircraft wings. Furthermore, the fluid "failure" has been taken as the visually-verified commencement of accumulation of snow on the fluid's surface or the loss of gloss of the fluid due to the formation of a thin layer of ice on the fluid in freezing fog, drizzle or rain situations. To the best of our knowledge, no scientific attempt has yet been made to correlate the visual failure criterion of a de- or anti-icing fluid following application to a flat plate or wing's surface with the degradation in aerodynamic performance of a near full-scale wing section caused by such fluids when contaminated by freezing precipitation.

## **Propulsion Wind Tunnel**

The experiments were performed in the National Research Council's Propulsion Wind Tunnel (Ref. 11). This facility is an open circuit wind tunnel with the fan at the entry, drawing air from and exhausting to the outdoors. The test section dimensions are 3 m (10 ft) wide by 6 m (20 ft) high by 12 m (40 ft) long. This design permits sub-freezing air to be drawn in during the Canadian winter, thereby simulating actual winter conditions in the test section. The 750 kW (1000 hp) electric fan drive used during these experiments can produce a maximum wind speed of  $44 \text{ m} \cdot \text{s}^{-1}$  (90 mph). A 6000 kW (8000 hp) gas turbine drive is also available. It can provide a maximum airspeed of about  $68 \text{ m} \cdot \text{s}^{-1}$  (140 mph).

## **Wing Model and Support**

The wing model used was a two-dimensional 1.52 m (5 ft) chord NACA 23012 aerofoil spanning the test section at approximately mid-height. An aerofoil with this cross-section and scale was chosen because it is representative of some commercial aerofoils (e.g. Cessna Citation Series 500 Executive Jet wing at 70% span). The aerofoil was supported at each end by a load cell mounted on the exterior of the test section wall (Figure 1).

Aerodynamic lift was determined from the combined output of the load cells. The drag was taken by drag links and the determination of the pitching moment (calculated about the quarter-chord point) was made possible by the configuration of the pitch mechanism at the port end of the aerofoil, Figure 1. Drag was not measured in the present tests. The aerofoil was pitched about a point very close to its quarter chord.

The aerofoil was constructed using 13 pine ribs equally-spaced on a 0.168 m OD tubular aluminum spar. This inner structure was covered by a continuous sheet of aluminum from the upper surface trailing edge around the leading edge to the lower surface trailing edge. Counter-sunk, flat-head wood screws held the aluminum sheet to the ribs, simulating the flush riveting typical of aircraft skins. In order to control the wing skin temperature and to simulate the cold-soaking of wing fuel tanks, a cold gas distribution system was added to the interior of the wing. Liquid nitrogen could then be injected into the distribution system resulting in the cooling of the skin's inner surface by the cold nitrogen gas. The wing temperature was determined from several resistance temperature detectors (RTDs) attached to various points on the inside of the wing's upper surface.

The Reynolds number ( $Re$ ) based on aerofoil chord ( $c$ ) was  $4.3 \times 10^6$  at the maximum wind speed of  $43 \text{ m} \cdot \text{s}^{-1}$ . This maximum wind speed was achieved following a simulated takeoff roll at an average acceleration of  $0.9 \text{ m} \cdot \text{s}^{-2}$ . While this was the maximum acceleration achievable by the electric motor drive, it was less than the ASTM recommended acceleration of  $2.1 \text{ m} \cdot \text{s}^{-2}$  for de-/anti-icing fluid aerodynamic testing for low rotational speed aircraft (Ref. 12). The typical maximum airspeed achieved in the tests was about  $3 \text{ m} \cdot \text{s}^{-1}$  above the range recommended by ASTM (30 to  $40 \text{ m} \cdot \text{s}^{-1}$ ).

The pitching rate achieved during the simulated aircraft rotation averaged just under  $1 \text{ deg} \cdot \text{s}^{-1}$  in these experiments. This was below the  $3 \text{ deg} \cdot \text{s}^{-1}$  that Ref. 13 states is a typical basis for certified takeoff performance, but nevertheless representative of the class of commercial aircraft.

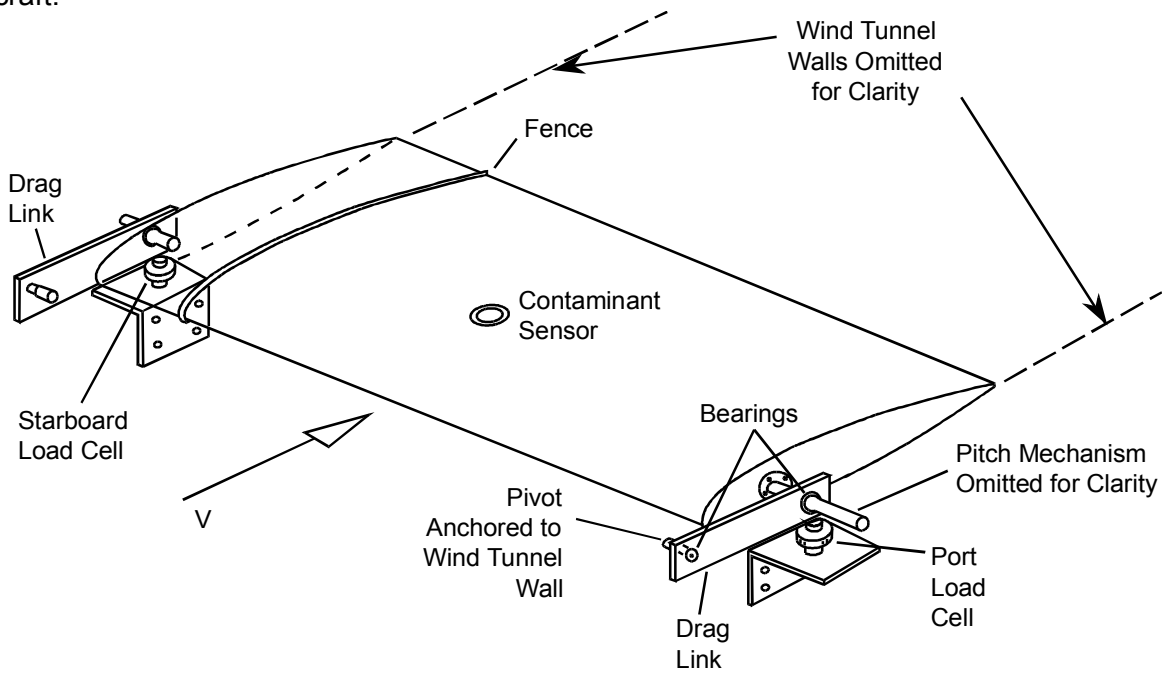


**Figure 1** A schematic diagram of the wing model used in the experiments

## **Instrumentation and Data Acquisition**

Data were acquired digitally for the following parameters: wind tunnel total and static pressures, total temperature, wing surface temperatures, wing pitch angle, wing lift load cell forces and the freezing rain sprayer water and air temperatures. Some of these data signals were low-pass filtered by 8 pole Bessel filters with a 3 dB cutoff frequency at 100 Hz prior to reaching the high-speed data acquisition system.

Digital data acquisition was performed by two IBM PC compatible microcomputers. The high-speed computer sampled 9 data channels at a rate of 550 Hz each. The data were then averaged for successive time periods of 7.3 ms thereby giving averaged values with an effective sampling rate of 137 Hz prior to being written to disk. The other computer sampled 14 channels at near 350 Hz prior to averaging down to approximately 1 Hz and writing the data to disk. This computer also performed calculations and displayed the results in real-time to enable monitoring of the experiment's progress.

The status of the de-/anti-icing fluids and the frozen precipitation on the wing were measured by a flush-mounted contaminant and fluid integrity sensor located near the mid-span of the model at 0.35 c. This system measures the admittance of the material above the sensor's surface (Ref. 14). By comparing these measurements with its previously acquired database, the system can distinguish between air, water, ice and FPD fluids, as well as provide warning of the imminent failure of the fluid caused by contamination with freezing precipitation. Previous testing of this sensor on SAE-standard flat plates was reported in Ref. 15.

Spot measurements of the fluid depth on the wing's upper surface were determined through the use of an NRC-developed laser-based, optical measurement system. Fluid wave characteristics were obtained by viewing wave crests superimposed upon a one centimetre high graduated chord-wise fence. In order to document the fluid run-off during the simulated takeoff run, two systems were used (Figure 2).

The first system utilized two 35 mm photographic cameras, one viewing the model from the test-section roof and the other from the side wall. The shutters of these cameras were synchronized to operate at one frame every two seconds for a total elapsed period of 72 s. Photography commenced just prior to the wing rotation. The side camera viewed wave motion against the fence (Figure 1) to determine mean wave height and, therefore, mean roughness height (e.g. Ref. 16). The other camera viewed wave motion from overhead to determine mean wave length, and hence mean roughness spacing. From these data, the dominant wave length was determined in the uncontaminated-fluid tests.

The other system was comprised of two video cameras, both viewing the model from the test-section roof. The upstream camera provided a full view of the aerofoil while the downstream camera (equipped with a telephoto lens) gave a close-up view of the laser spot and the refractive light ring produced by a layer of fluid or ice. Data from the laser system provided corroborative evidence of wave height.

## **Fluid Application**

SAE Type II anti-icing fluids are pseudoplastic materials which exhibit non-Newtonian flow behavior. As a result, special care must be taken when storing and applying these fluids so that the viscosity upon application to a wing's surface has not degraded by more than 20% from the



manufacturer's standard value. Airline-standard pumps and nozzles were not considered to be appropriate considering the short length of the wing model (1.5 m or 5 ft). For these experiments, a spreading wand was attached to a pressurizable reservoir to enable fluid application. As shown in Figure 3, this device provides rapid and uniform application of the fluids. In order to confirm that this application method did not over-shear the fluid, thereby seriously decreasing its viscosity upon application, a viscometer was used to measure the fluid viscosity prior to and following fluid application. The procedure used was that recommended in ASTM Standard Method D 2196-86. The fluids were either dyed by the manufacturer, or just prior to each experiment using standard food color dyes to enhance the visibility of the fluid flow during the simulated takeoff roll.

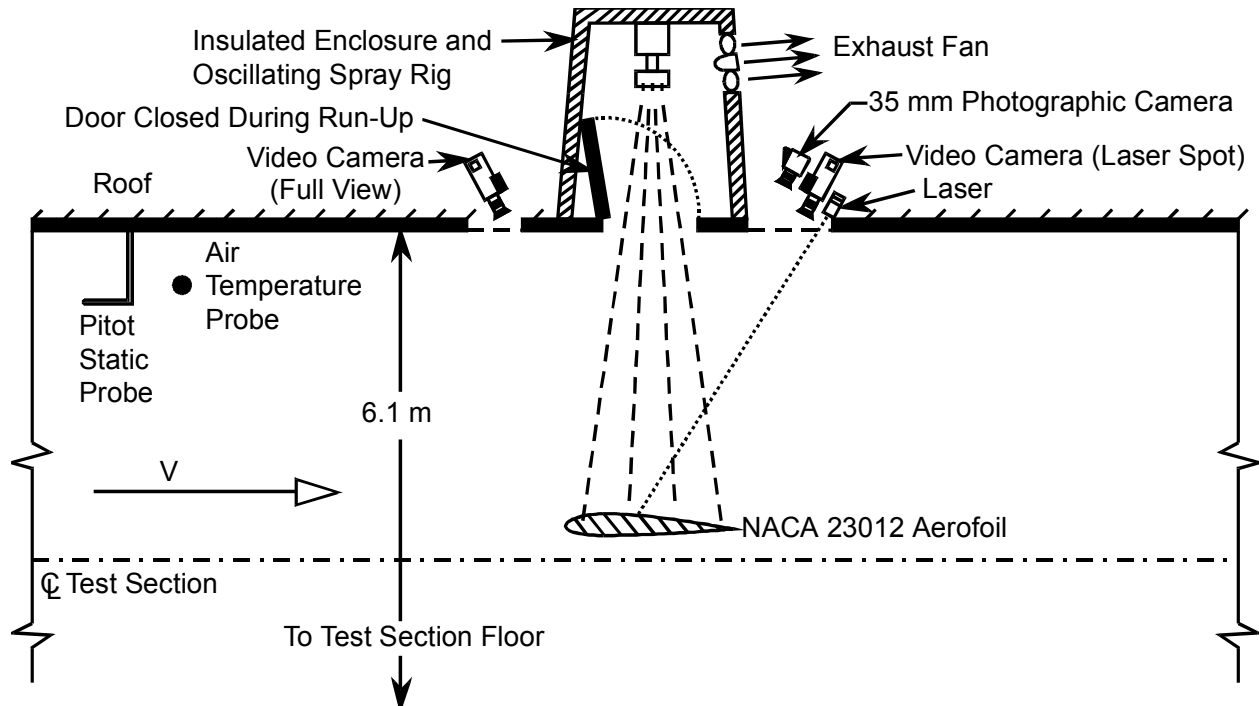


**Figure 2** A schematic view of the upper half of the test section showing the location of the wing model, the freezing rain simulator and the photographic systems

## Freezing Precipitation Simulation

Freezing precipitation (applied to the model prior to the simulated takeoff) was created using an oscillating spray device located in an enclosure mounted above the test section (Figure 2). This NRC-developed sprayer utilizes two 20 gauge hypodermic syringe needles to create fine streams of water which naturally break up into droplets after a fall of several meters. Two small air jets impinging upon the water jet further assist the droplet breakup, and produce a drop size distribution with a median volume diameter of about 1.3 mm, which is typical for rain. By pre-cooling the air and water to just above 0°C, the droplets become slightly supercooled following their fall of over 4 m to the wing's surface when the air temperature is sub-freezing. In those cases where the air temperature is above 0°C, cooling of the wing's interior permits experiments which simulate rain on a cold-soaked wing. By scanning the spray head in a Lissajous pattern, the area coverage is increased to approximately 5 m<sup>2</sup> and the rainfall intensity is controlled at a value  $35 \pm 5 \text{ g} \cdot \text{dm}^{-2} \cdot \text{h}^{-1}$  over all of the wing's surface except within

about 30 cm from each wall. This corresponds to a moderate freezing rain rate. A trap door in the test section roof could be opened during the precipitation contamination phase of an experiment, and then closed once the freezing rain had ended so as to provide a smooth wind tunnel ceiling during the aerodynamic testing.

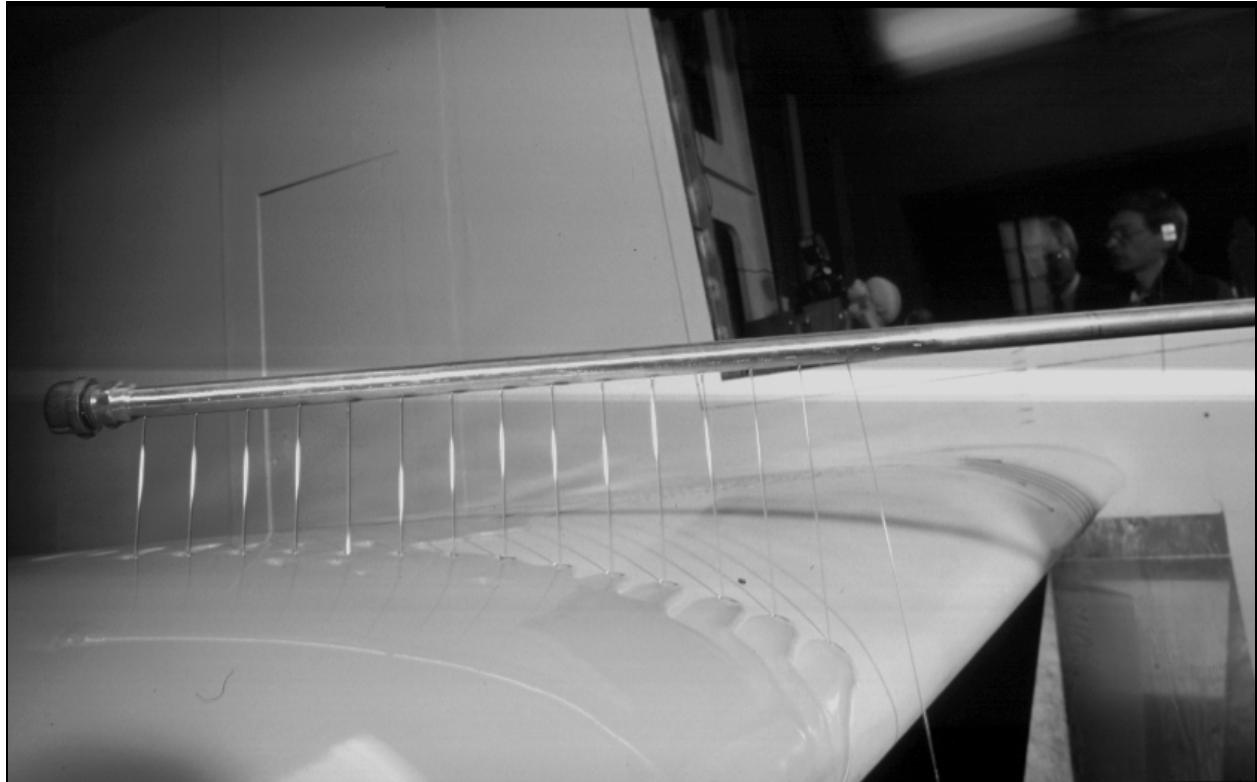


**Figure 3** The wand-like device used for evenly spreading the de- and anti-icing fluids on the wing

## Flow Visualization

Flow visualization experiments using wool tufts were carried out for the purpose of identifying regions on the model's upper surface where the flow was three-dimensional. For angles of attack ( $\alpha$ ) less than or equal to 12 deg, the flow on the upper surface was found to have small wedges of unsteadiness adjacent to the wall only, with the remainder of the upper surface being fully attached, steady and two-dimensional. For  $\alpha > 12$  deg, as the aerofoil approached the stall, these wedges developed into fully separated flow, their width reaching a maximum of 15% of model span at the trailing edge. In this range of  $\alpha$ , the slight upper surface discontinuity caused by the contaminant and fluid integrity sensor created a small wedge of unsteadiness and for the highest angles this wedge developed into a region of separation for the last 20% of chord. Since there was no treatment of the wall boundary layers, the flow became highly three-dimensional above the stall ( $\alpha \approx 17$  deg). Here the outer 15% of span at the wall reverted to what appeared to be fully attached flow, while the inner 70% was fully separated from at least 16.7%  $c$  (the first span-wise line of tufts) to the trailing edge. This three-dimensional behavior of the upper surface flow would be expected to produce a somewhat reduced lift curve slope in these experiments.

## Experiment Matrix

In order to meet the objectives of this feasibility study, four types of experiments were run in the PWT. These experiments are summarized in Table 1. In this table, the second column identifies the type of experiment and the third column the fluid type and concentration. The codes for this latter column indicate SAE Type I or II fluids from manufacturer A or B applied with a dilution of 100/0, 75/25 or 50/50 fluid/water. The wing temperature is representative of the mean value over the leading half of the wing. The “Ice Visible” column indicates the time at which ice was first visually detected on the wing, not necessarily near the contaminant and fluid integrity sensor. The “Sensor Contamination Indication” column shows the earliest time at which the contaminant and fluid integrity system reported either a failing fluid, failed fluid or ice/snow.

**Table 1** Time Elapsed Following Fluid Application (min)

Expt. ID.	Expt. Type	Fluid Type	Air Temp. (°C)	Wing Temp. (°C)	Time Elapsed Following Fluid Application (min)					Max. Lift Coeff. Change (%)	Stall Angle Change (deg)
					Freezing Rain Start	Freezing Rain Stop	Ice Visible	Sensor Contamination Indication	Takeoff Run		
29F	Clean		7.5	8.4							
30A	Clean		3.4	5.6						0.0	0.0
23A	Fluid	IIA 100/0	3.9	6					13		
27C	Fluid	IIA 75/25	0	-0.3					24		
30H	Fluid	IIA 75/25	8.1	1.4					27	-0.6	-0.2
27D	Fluid	IIA 50/50	1.6	-0.4					23		
29E	Fluid	IIB 100/0	6.6	5.1					12		
29D	Fluid	IIB 50/50	5.6	1.4					13	0.0	0.4
24B	Ice		0.1	-2.4	0	6	1	1	23		
28B	Ice		1.1	-5.5	0	5	0		10	-18.0	-5.1
28C	Ice		1.8	-1.3	0	5	0		26	-17.5	-5.2
29C	Ice		3.7	-2.4	0	12	0	22	23	-2.6	-0.1
30F	Fluid/Ice	IA 100/0	5.9	-4.1	2	27	18	14	42	-0.8	-1.2
25A	Fluid/Ice	IB 100/0	-2.4	-2	12	59	22	35	71		
29B	Fluid/Ice	IIA 100/0	1.5	-0.9	22	114	82	124	127	-3.9	-1.8
28A	Fluid/Ice	IIA 75/25	-0.9	-0.6	15	88	75	37	98	-9.8	-3.3
25D	Fluid/Ice	IIA 50/50	1.8	-0.5	10	47		28	59		
24A	Fluid/Ice	IIB 100/0	-1.8	-2.8	6	125	70	42	135		
27A	Fluid/Ice	IIB 75/25	-1.9	-1.6	8	49	43	24	60		
27B	Fluid/Ice	IIB 50/50	-1.5	-1.5	6	36	21	9	47		
30D	Frost		3.8	-0.5		95	5	111	105	-18.6	-4.5
30E	Frost		3.8	-0.5		95	5	111	105	-8.7	-3.4

First, two experiments were performed with a clean, uncontaminated wing model. The results of these experiments were compared to published data for a NACA 23012 aerofoil (Ref. 17). They were also used as a baseline against which the results from the other experiments were compared. Next, six experiments were run with only de- or anti-icing fluid on the wing. Then two simulated takeoff experiments were carried out in which freezing rain produced a contamination of the wing model’s upper surface. Following this, eight runs were made where a de- or anti-icing fluid was applied and then contaminated by freezing rain. Finally, two experiments were performed to determine the aerodynamic effects of a thin layer of frost.

## Clean Wing Aerodynamics

Figure 4 is a plot of lift coefficient ( $C_L$ ) and moment coefficient ( $C_m$ ) vs.  $\alpha$  for the clean aerofoil at  $Re = 4.3 \times 10^6$ . The moment coefficient is referenced to the aerofoil's quarter-chord point. These coefficients have not been corrected for wall interference. As mentioned in the section on model support, drag was not measured and so wake blockage could not be calculated. Noting that the ratio of airfoil chord to test section height ( $c/h$ ) was 0.25, the corrections due to solid and wake blockage are estimated to be less than 2% for angles of attack below the stall.

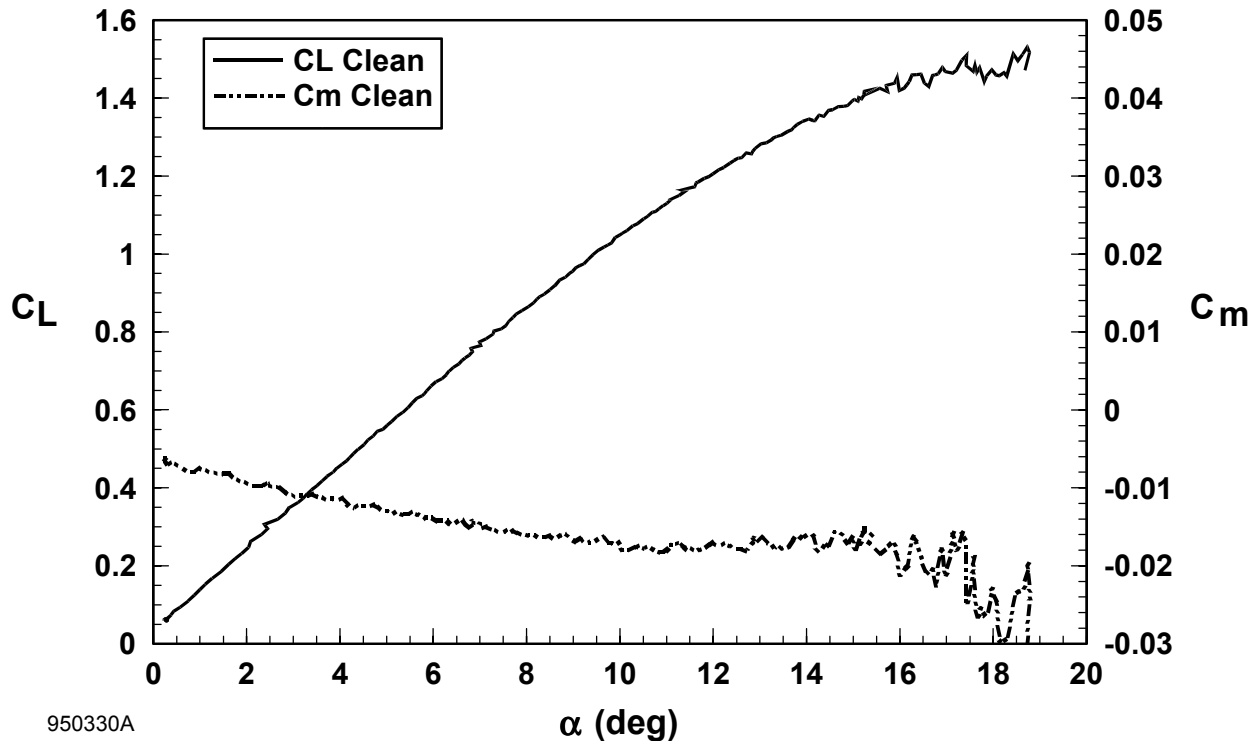


**Figure 4** Lift and moment coefficients vs. angle of attack for a clean wing

When the data of Figure 4 are compared with Ref. 17 for the NACA 23012 at  $Re = 3.0 \times 10^6$ , the lift curve slope of the present experiment is found to be smaller than the two-dimensional counterpart. The lift curve slope of Ref. 17 for the NACA 23012 is constant at 0.106 per degree for  $\alpha \leq 10$  deg with a slight decrease for  $\alpha > 10$  deg. The present experiment exhibits a lift curve slope of 0.106 up to  $\alpha = 5$  deg, reducing to 0.073 at  $\alpha = 12$  deg and 0.04 as the model approaches the stall. As mentioned in the section on flow visualization, the upper surface flow developed regions of three-dimensionality for  $\alpha > 12$  deg and this is taken to be the reason for the reduction in lift curve slope. The level of three dimensionality can be quantified to some degree by an effective aspect ratio. Computations with a 3-D panel code indicate that the clean wing behaves, in respect to its lift coefficient, as a wing with an aspect ratio of 19 at  $\alpha = 10$  deg.

Finally, there is an indication of a constant offset of +1 deg in the measurement of  $\alpha$  for the complete experimental programme. This is thought to be the result of a mechanical misalignment of the aerofoil's chord line with the test section centre line.

In other respects the curves of  $C_L$  and  $C_M$  vs.  $\alpha$  compare favourably with Ref. 17 and thereby indicate confidence in the apparatus used to determine the aerodynamic loads. For the remainder of this paper,  $C_{L\text{Max}}$  refers to the maximum lift coefficient obtained when the wing was clean.

### De-/Anti-Icing Fluid Flow Behaviour and Its Aerodynamic Effects

Wave height and spacing were photographed in each fluid flow test as the wind tunnel speed increased beyond  $20\text{ m}\cdot\text{s}^{-1}$  and throughout and beyond the pitch-up phase at  $43\text{ m}\cdot\text{s}^{-1}$ . Some corroborative data were also obtained by photographing the optical fringe pattern of the laser beam in the fluid surface. When the above data were analyzed, it was discovered that the average wave height ( $k$ ) as well as the average ratio of wave spacing to height ( $\lambda$ ) were not only nearly identical in all five run-back tests analyzed, but that these statistics were approximately uniform over the downstream half of the aerofoil. The measured values of  $k$  and  $\lambda$  were  $0.45 \pm 0.05\text{ mm}$  and  $38 \pm 6$ , respectively.

Of the six experiments of this type performed, only two were taken to the point of aerofoil stall. The  $C_L$  and  $C_m$  curves for one of these experiments are displayed in Figure 5. In Cases 30H and 29D, there was less than a 0.5 deg change in the stall angle as compared to the clean wing case and the maximum lift coefficient change ( $\Delta C_{L\text{Max}} / C_{L\text{Max}}$ ) was less than 1%. These results compare favorably to those reported in Ref. 4, where lift coefficient losses of 5% or less were found at 0 C.

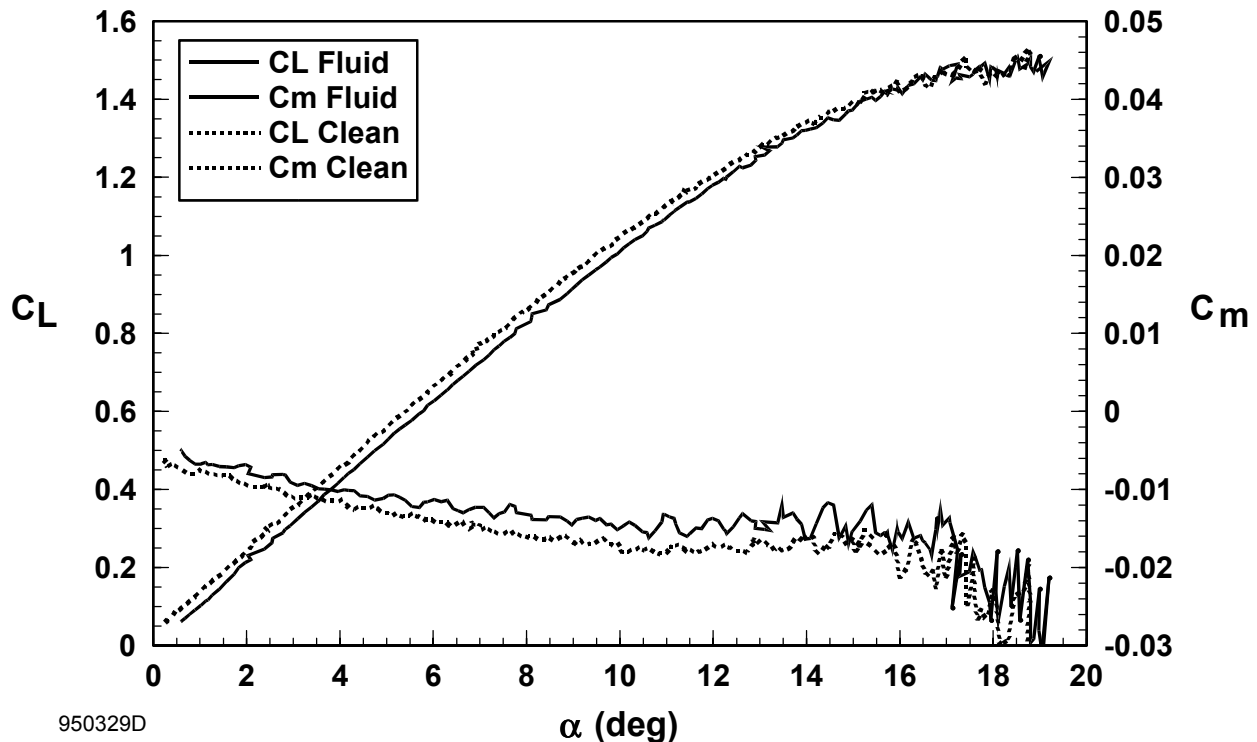


**Figure 5** Lift and moment coefficients vs. angle of attack for a Type II fluid diluted 50/50

## Aerodynamic Effects of Freezing Precipitation

In three of the four freezing precipitation experiments, the wing was pitched up to the point of aerofoil stall. In one case (29C), there was only a marginal loss of maximum lift, and virtually no change in stall angle. In the other two cases (28B and 28C), the  $\Delta C_{L\text{Max}} / C_{L\text{Max}}$  was near -18% with a decrease in stall angle ( $\Delta\alpha_{\text{Stall}}$ ) of near 5 deg (see Figure 6). While the air temperature was higher for Case 29C (3.7°C) than for the other two (1.1 and 1.8°C), the wing surface temperatures for all three experiments were below 0°C. Examination of the photographs of the ice surface indicates that the ice covering the wing just prior to the takeoff run of Case 29C was smoother than that for the other two experiments. This difference in ice surface roughness may be attributed to a lower rate of freezing at the higher ambient temperature.

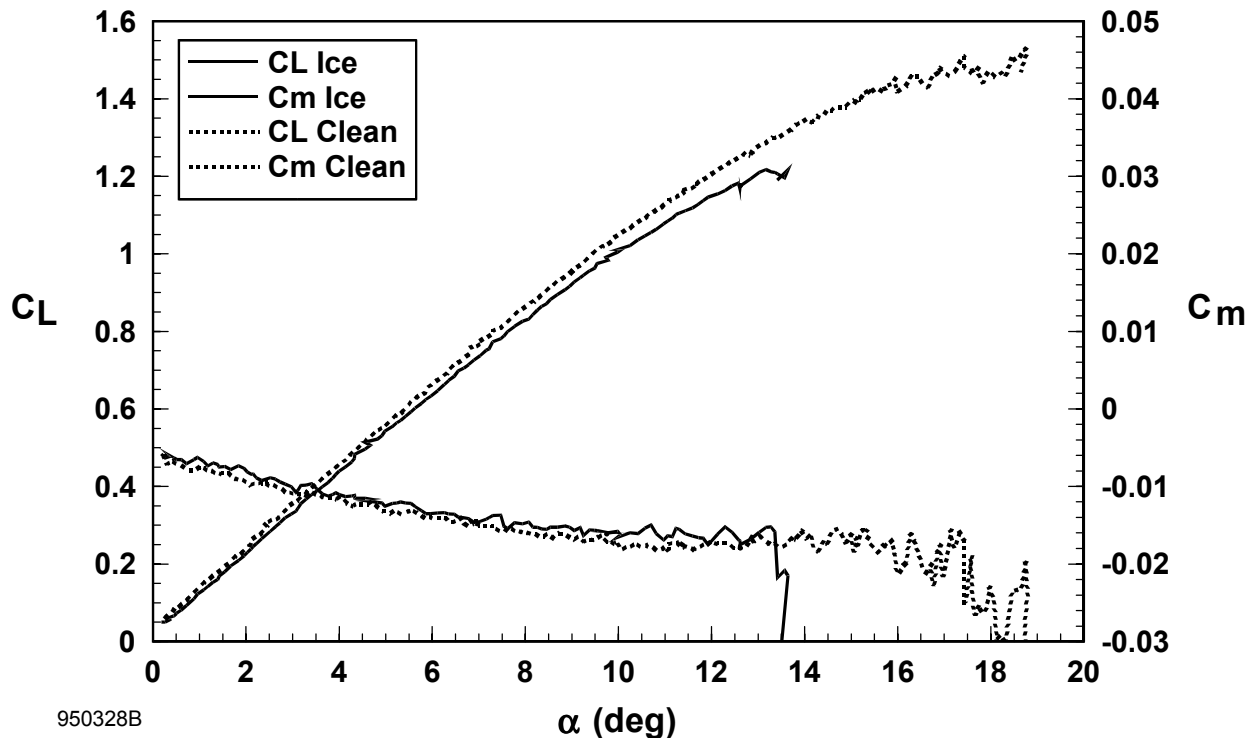


**Figure 6** Lift and moment coefficients vs. angle of attack for a layer of ice formed by rain on a cold-soaked wing

## Aerodynamic Effects of Freezing Precipitation on De-/Anti-Icing Fluids

A total of eight experiments was performed with a de- or anti-icing fluid contaminated by simulated freezing rain. In three of these (Cases 30F, 29B and 28A), the wing was pitched to the stall angle.

The  $C_L$  and  $C_m$  curves for Case 29B are shown in Figure 7. In these cases, the  $\Delta C_{L\text{Max}} / C_{L\text{Max}}$  varied between -1 and -10% while the  $\Delta\alpha_{\text{Stall}}$  varied between -1 and -4 deg. The smallest change occurred with Case 30F, where an SAE Type I fluid had been applied. The ambient air temperature in this latter case was +5.9°C, substantially warmer than the other two cases (1.5 and -0.9°C). Once again, this suggests that the effect of ambient temperature is significant.

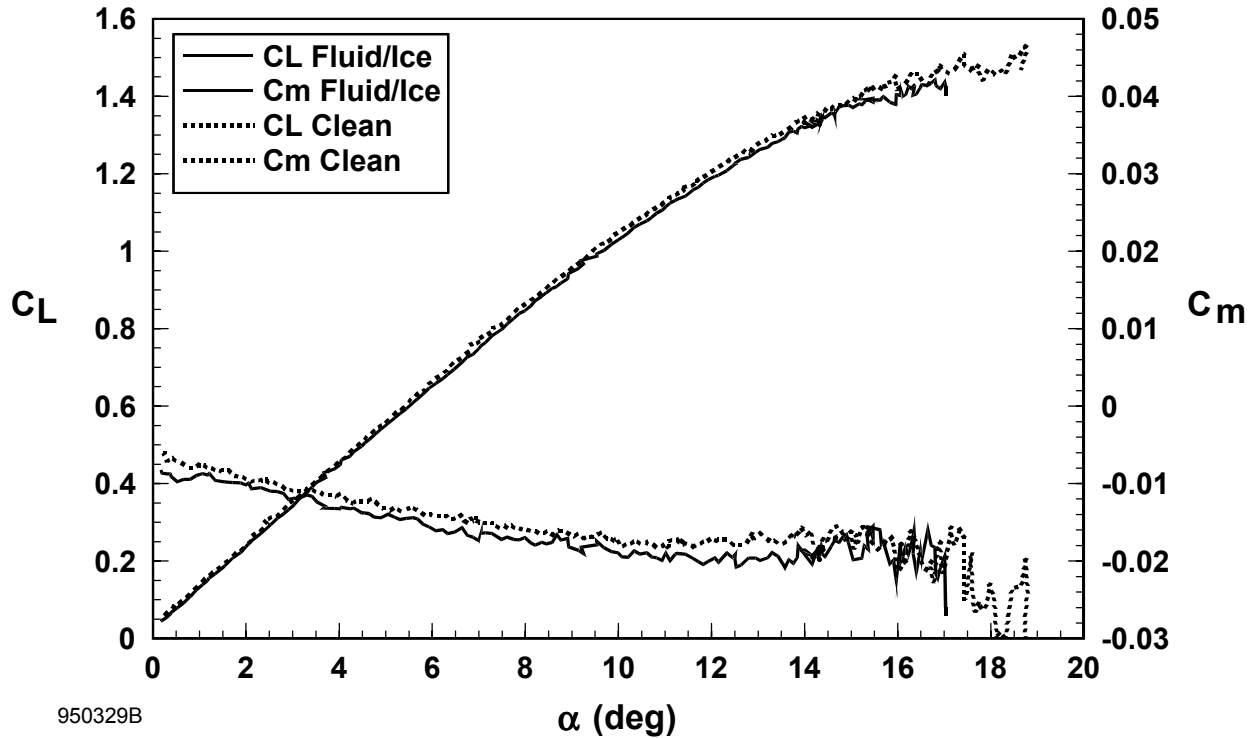


**Figure 7** Lift and moment coefficients vs. angle of attack for a layer of ice formed following the failure of a layer of neat Type II fluid

The SAE Holdover Time (period of protection provided by the FPD fluid) for a Type I fluid under freezing rain conditions for temperatures above 0°C is 2 to 5 min. Table 1 shows that the simulated freezing rain continued for a period of 25 min in this case, well beyond the point of a failure indication from the contaminant and fluid integrity sensor, which occurred at 14 min. Despite this, the resulting layer of ice did not have a major impact on the wing's lift. In Case 29B, a Type II fluid was applied at a 100/0 concentration. The holdover time for this case, where the air temperature was +1.5°C, is given as 8 to 20 min. The simulated rain continued for a period of 92 min and ice was visible 82 min after fluid application. The takeoff run began 127 min following fluid application. Finally, in Case 28A, a Type II fluid was applied at a 75/25 concentration, providing a holdover time of 8 to 20 min for temperatures between 0 and -7°C. The contaminant and fluid integrity sensor indicated fluid failure at 37 min, but the freezing rain continued for a period of 73 min. These two cases also show that at these temperatures, the slow dilution of the FPD combined with the long period to the point of freezing, appears to produce a layer of ice sufficiently smooth that the impact on the aerodynamics is not severe.

In all of these cases, the contaminant and fluid integrity sensor provided an indication of fluid failure prior to the takeoff run. In some cases, this indication came before ice was seen to be forming on the wing's surface, but in other cases, ice formed on some part of the wing prior to the provision of a warning. In no case, however, was ice observed on the sensor prior to a warning indication.

## Aerodynamic Effects of Frost Formation

Finally, as a basis for comparison with the contaminated fluid experiments, two runs were made following a period of frost formation on the wing. The frost was created by injecting cold nitrogen into the wing, thereby simulating a cold-soaked fuel situation. As noted in Table 1, the air temperature was near  $+4^{\circ}\text{C}$  while the wing's surface temperature was at  $-0.5^{\circ}\text{C}$  or below. Figure 8 shows the  $C_L$  and  $C_m$  curves for these two cases. Case 30D was run first, and resulted in a maximum lift coefficient change ( $\Delta C_{L \text{ Max}} / C_{L \text{ Max}}$ ) of near -19% and a decrease in stall angle of 4.5 deg. Following this experiment, during which some sublimation of the frost surface had occurred, another run was made (Case 30E). The curves for this case are labeled as "Light Frost" in Figure 8. They show a reduced  $\Delta C_{L \text{ Max}} / C_{L \text{ Max}}$  (-9 vs. -19%) and  $\Delta \alpha_{\text{Stall}}$  (-3.4 vs. -4.5 deg).

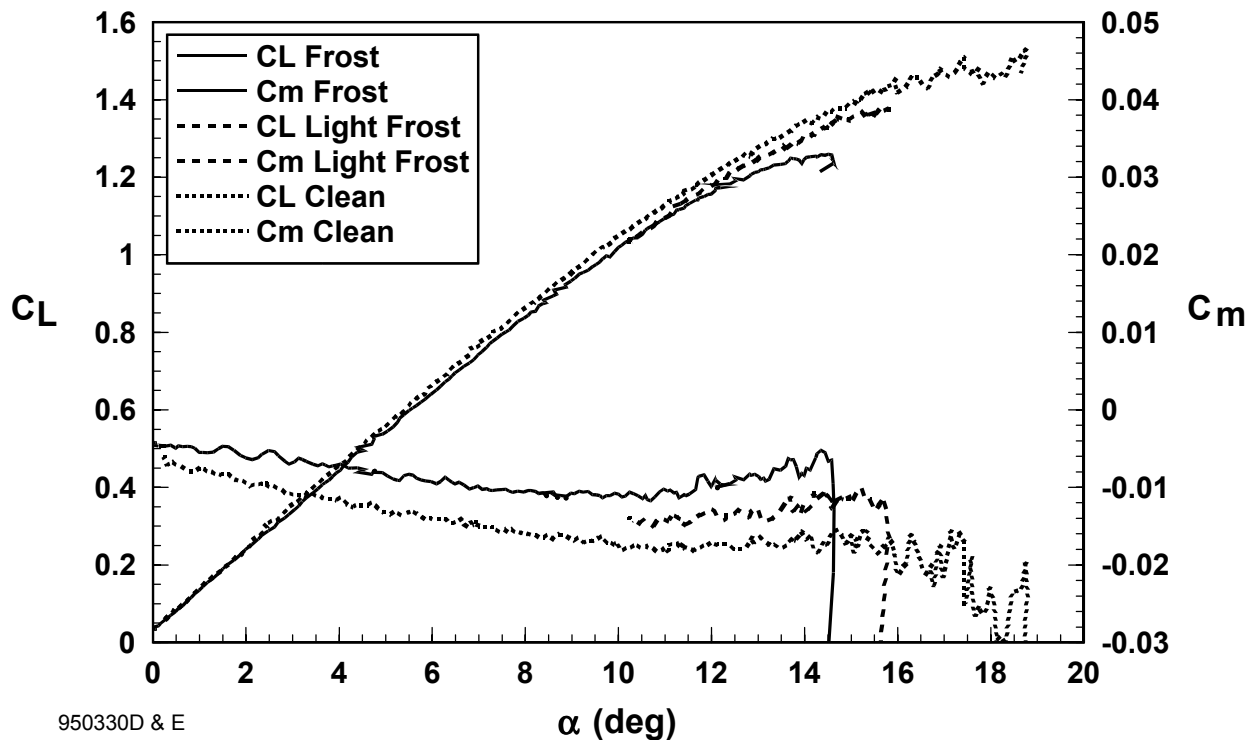


**Figure 8** Lift and moment coefficients vs. angle of attack for a layer of frost and a partially sublimated layer of frost (labelled Light Frost)

## Summary of Aerodynamic Effects

Summaries of the changes in maximum lift coefficient ( $\Delta C_{L \text{ Max}} / C_{L \text{ Max}}$ ) and stall angle ( $\Delta \alpha_{\text{Stall}}$ ) for each of the cases previously discussed are presented in Figures 9 and 10, respectively. Ambient and wing-surface temperatures are shown, respectively, for each case. In these experiments, the loss in lift coefficient for uncontaminated fluids at temperatures near  $0^{\circ}\text{C}$  were less than 1% and the stall angle changed by less than 1 deg. In contrast, ice formed by freezing rain or rain on a cold-soaked wing, or by frost formation on a cold-soaked wing resulted in lift coefficient losses as large as 18.6% and stall angle reductions of up to 5.2 deg. Ice forming on de- and anti-icing fluids following their failure to further protect the wing's surface



(beyond the fluids' holdover time) resulted in changes in the lift coefficient of up to -9.8% and in stall angle of up to -3.3 deg.

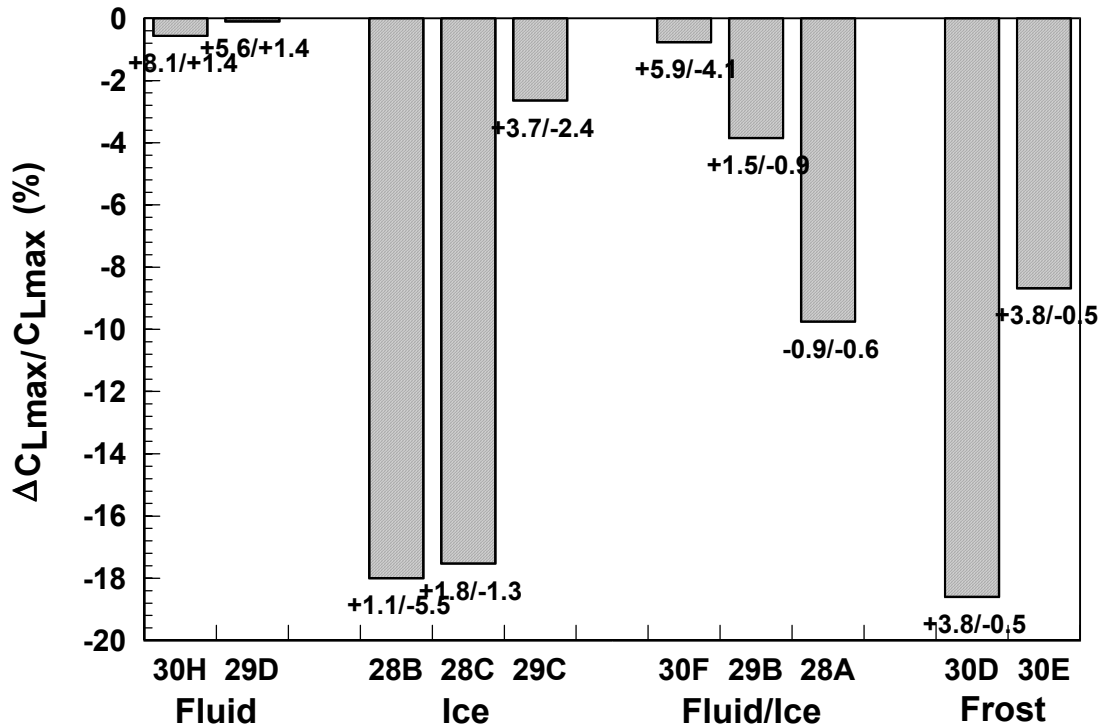


**Figure 9** Changes in the maximum lift coefficient as a function of wing contaminant and air and wing temperatures

Lift loss due to contamination, which, in the present case, is measured on the complete wing, is generated mainly in the high shear regions. Moreover, representative fluid runoff characteristics are confined to regions free of end effects. Therefore, to relate the measured characteristics summarized in Figures 9 and 10 to actual flight, the results should be corrected to the equivalent aspect ratio. Estimates for a clean wing showed that the effective aspect ratio decreases in the vicinity of stall. Thus, the lift losses estimated based on the active portion of the wing are substantially larger than the values given in Figures 9 and 10.

## Conclusions

A series of experiments performed in NRC's 3 m x 6 m open-circuit Propulsion Wind Tunnel during the winter of 1994-95 on a 1.5 m chord two-dimensional wing model leads to the following conclusions:

The flow of de- and anti-icing fluids on the wing model during the simulated takeoff roll and rotation develops waves of near 0.5 mm height and non-dimensional spacing of 38. The fluids do not cause a lift coefficient loss of more than 1% at temperatures near freezing.

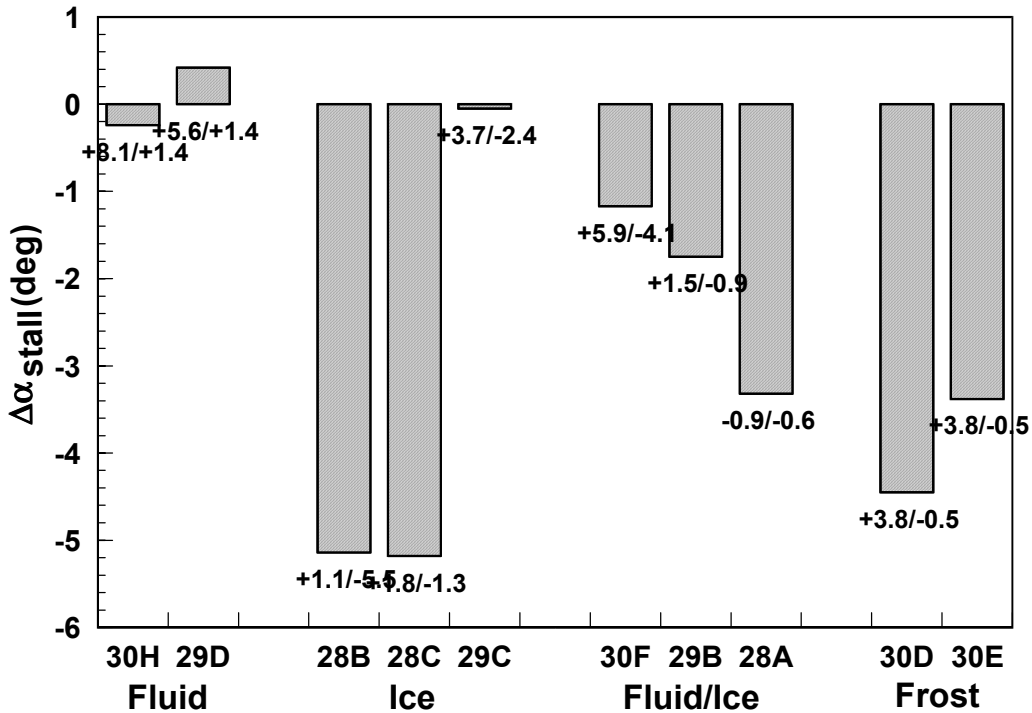


**Figure 10** Changes in the stall angle as a function of wing contaminant and air and wing temperatures

The layer of ice formed on the wing's upper surface following a period of simulated freezing rain or rain on a cold-soaked wing can produce a range of aerodynamic effects. It appears that ice which forms relatively slowly as a result of rain on a cold-soaked wing has minimal impact. On the other hand, the ice formed by simulated freezing rain, which appeared to have a rougher surface, led to a lift coefficient loss as large as 18% and a stall angle reduction of up to 5.2 deg.

The ice which formed with de- or anti-icing fluids following the failure of the fluid to protect the wing caused maximum lift coefficient losses as high as 9.8% and reductions in stall angle by as much as 3.3 deg. Here again, the ambient temperature appeared to influence the ice surface texture and thus the aerodynamic impact.

A thin layer of frost grown on a simulated cold-soaked wing resulted in a lift loss of up to 18.6% and a reduction in stall angle of up to 4.5 deg. Once the frost had partially sublimated during the first simulated takeoff run, the following run demonstrated less aerodynamic penalty. Even though the frost formed a uniformly thin coating on the wing, the small-scale roughness of its surface appeared to significantly impact the airflow about the wing.

The significant aerodynamic impacts found in some of these experiments suggests that these experiments should be extended by utilizing a commuter-class aerofoil with a flap and that the range of environmental conditions should be extended, including colder ambient temperatures and simulated snowfall.

## References

1. Moshansky, V.P., "Commission of Inquiry into the Air Ontario Crash at Dryden, Ontario (Canada), Final Report", Minister of Supply and Services Canada, 1992.
2. van Hengst, J., "Flight Tests of the Aerodynamic Effects of Type I and Type II Ground De-/Anti-Icing Fluids on the Fokker 50 and Fokker 100 Aircraft", AIAA Paper 91-0785, Jan 1991.
3. Munafo, C.F., and Masters, C.O., "Evaluation of The Aerodynamic Effects of Commuter Class (Type 1 1/2) Anti-Icing Fluids on Small General Aviation Airplanes", AIAA Paper 92-0643, Jan 1992.
4. Carbonaro, M., and Cunha, F., "Aerodynamic Effects of De/Anti-icing Fluids and Criteria for Their Aerodynamic Acceptance", SAE Aircraft Ground Deicing Conference Transcription of Presentations, Salt Lake City, Utah, Jun 1993.
5. Runyan, L., Zierten, T., Hill, E., and Addy, H., "Lewis Icing Research Tunnel Test of the Aerodynamic Effects of Aircraft Ground Deicing/Anti-Icing Fluids", NASA Technical Paper 3238, 1992.
6. Ellis, N.D., "Aircraft Ground De-Icing/Anti-Icing Fluids Aerodynamic Evaluation", SAE Aircraft Ground Deicing Conference Transcription of Presentations, Salt Lake City, Utah, Jun 1993.
7. Kotker, D., "Aerodynamic Effects Related to Aircraft Icing While on the Ground", SAE Aircraft Ground Deicing Conference Transcription of Presentations, Salt Lake City, Utah, Jun 1993.
8. APS Aviation Inc., "Results of Fluid Holdover Time Tests in Canada", SAE Aircraft Ground Deicing Conference Transcription of Presentations, Salt Lake City, Utah, Jun 1993.
9. Oleskiw, M.M., "Freezing Fog and Frost Simulation Tests in Canada", SAE Aircraft Ground Deicing Conference Transcription of Presentations, Salt Lake City, Utah, Jun 1993.
10. Kuperman, M.H., and Moore, R.K., "Deicing/Anti-Icing Fluid Holdover Time Measurements Aircraft and Frosticator Panel Correlation - Snow Conditions", SAE Aircraft Ground Deicing Conference Transcription of Presentations, Salt Lake City, Utah, Jun 1993.
11. Williamson, R.G., "NRC Propulsion Wind Tunnel", NRC Publication Series on Transportation, Vol.12, No.2, Sep 1980.
12. SAE Aerospace Material Specification (AMS) 1428, Appendix B.
13. R.E. Brumby, R.E., "The Effects of Wing Ice Contamination on Essential Flight Characteristics", 68th AGARD Fluid Dynamics Panel Specialists Meeting on Effects of Adverse Weather on Aerodynamics, Toulouse, France, Apr 1991.
14. Inkpen, S., Brobeck, C. and Nolan, C., "Development of a Sensor for the Detection of Aircraft Wing Contaminants", AIAA Paper 92-0300, Jan 1992.

15. Oleskiw, M.M., "Laboratory Evaluation of a Sensor for Detection of Aircraft Wing Contaminants", AIAA Paper 92-0301, Jan 1992.
16. Wu, J., "Laboratory studies of wind-wave interactions", *Journal of Fluid Mechanics*, Vol 34, Part 1, 1968.
17. Abbott, I.H., and von Doenhoff, A.E., *Theory of Wing Sections Including a Summary of Airfoil Data*, Dover Publications, Inc., New York, 1959.